

Synthesis, crystal structure and electroluminescent properties of *fac*-bromotricarbonyl([1,2,5]oxadiazolo[3',4':5,6]pyrazino[2,3-*f*][1,10]phenanthroline)rhenium (I)

Ilya V. Taydakov,^{*a,b} Andrey A. Vashchenko,^a Konstantin A. Lyssenko,^b Lidia S. Konstantinova,^{c,d} Ekaterina A. Knyazeva,^{c,d} and Natalia V. Obruchnikova^c

^a*P. N. Lebedev Institute of Physics, Russian Academy of Sciences, 119991 Moscow*

^b*A. N. Nesmeyanov Institute of Organoelement Compounds, Russian Academy of Sciences, 119991 Moscow*

^c*N. D. Zelinsky Institute of Organic Chemistry, Russian Academy of Sciences, 119991 Moscow*

^d*Nanotechnology Education and Research Center, South Ural State University, 454080 Chelyabinsk, Russia*

E-mail: taidakov@gmail.com

Dedicated to Prof. Oleg A. Rakitin on the occasion of his 65th birthday

Received 04-08-2017

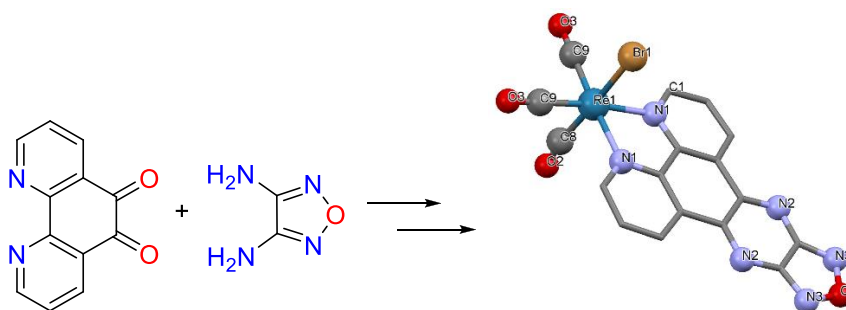
Accepted 06-12-2017

Published on line 07-09-2017

Dates to be inserted by editorial office

Abstract

An efficient and simple synthetic protocol has been developed for preparation of [1,2,5]chalcogenadiazolo[3',4':5,6]pyrazino[2,3-*f*][1,10]phenanthrolines. The first Re(I) bromotricarbonyl complex bearing [1,2,5]oxadiazolo[3',4':5,6]pyrazino[2,3-*f*][1,10]phenanthroline as a ligand was synthesized. Crystal structure of complex and free ligand, photo- and electroluminescent properties of *fac*-bromotricarbonyl ([1,2,5]oxadiazolo[3',4':5,6]pyrazino[2,3-*f*][1,10]phenanthroline)rhenium (I) were investigated.



Keywords: Chalcogenadiazoles, fused oxadiazoles, rhenium (I) bromocarbonyl complexes, luminescence, OLED.

Introduction

Metallorganic complexes of noble and rare metals are widely used in modern technology.¹⁻² Among all, complexes of Ir(III), Pt(II), Ru(II) and Os(II) are the most popular materials for solar cells and OLED (Organic Light Emitting Diode) applications.³ Electronic structure of Re(I) complexes is similar to those elements, but its coordination chemistry is much less explored.⁴⁻⁵

Heavy atom assisted spin-orbit coupling effect, which is common for complexes of heavy *d*-elements, brings to mixing of triplet and singlet states in excited complex. This mixing has resulted in intensive phosphorescence, because in this case $T_1 \rightarrow S_0$ transitions became partially allowed.⁶ The first observations of red emission of Re(I) complexes was made by Wrighton and Morse⁷ in 1974 for compounds of general composition $[\text{ReCl}(\text{CO})_3(\text{L})]$, where L – heterocyclic diimine ligand such as 1,10-phenanthroline (Fig.1, **1**). The most of luminescence observation has been made for complexes with similar structures.

The first example of OLED structure with active layer based of Re(I) complex has been prepared in 1999,⁸ in these devices mixtures of several simple complexes with polycarbonate (host material) were used. The maximum intensity of electroluminescence was about 700 cd/m² and spectral maximum of emission was situated around 670 nm (deep-red color). In the recent years, electroluminescent performance of Re(I)-based OLED was significantly improved due to utilization of more sophisticated ligands bearing extended chromophore system; for example, the complexes with polyarylated 1,10-phenanthroline (**2**),⁹ 2-(pyridyl)benzimidazole (**3**)¹⁰ and 2,3-diphenylpyrazino[2,3-*f*][1,10]phenanthroline (**4**)¹¹ were tested (Figure 1). It was quite logically to combine properties of ligands **3** and **4** by introducing an chalcogenadiazole fragment into molecule of pyrazino[2,3-*f*][1,10]phenanthroline. One can assume that such a new ligand will combine good charge-transfer properties of aryl substituted diazoles with strong coordination ability of phenanthroline moiety. The most promising ligands for OLED applications are shown in the Figure 2.

To the best of our knowledge, only a few examples of such types of compound were reported. In particular compound **5a** - [1,2,5]oxadiazolo[3',4':5,6]pyrazino[2,3-*f*][1,10]phenanthroline has been synthesized by Peng *et al.*¹² by interaction of 1,10-phenanthroline-5,6-dione and 3,4-diaminofurazan in HCl-EtOH mixture with overall yield about 31 % after purification by chromatography. Neither thiadiazole (**5b**) nor selenadiazole (**5c**) derivatives were described in literature up to date. Coordination chemistry of ligand **5a** has been very confined – only two complexes with $\text{Ru}(\text{bipy})\text{Cl}_2$ (bipy - 2,2'-bipyridine)¹² and two - with $\text{Ru}(\text{tpy})\text{Cl}_3$ (tpy - 2,2':6',2''-terpyridine)¹³ were prepared and characterized. All compounds have been used as fluorescent probes for DNA. In this communication, we report improved synthetic approach to compounds **5a** and **5b** and first successful utilization of Re(I) bromocarbonyl complex with ligand **5a** as an active layer of simple OLED structure.

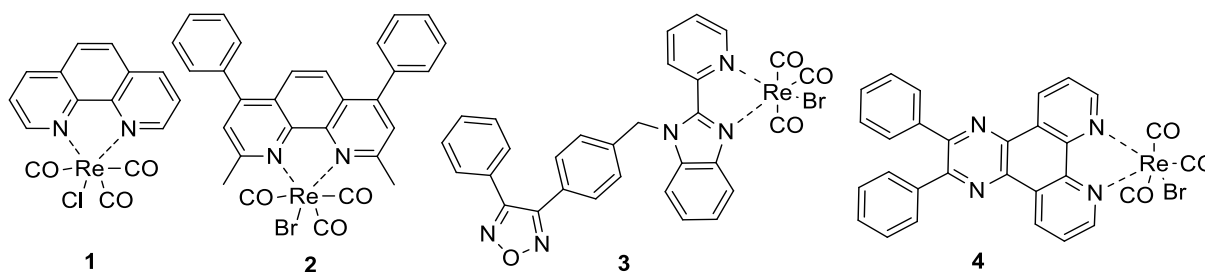


Figure 1. Some Re(I) halocarbonyl complexes with bidentate *N,N*-ligands.

X-ray structure. Single crystals of **5a** and **9a**, suitable for X-ray diffraction (XRD) experiments were obtained by slow diffusion of EtOH vapor into saturated solution of complex in DMSO. The crystal structure of **5a** was reported previously at room temperature. According to XRD at 120 K the single crystal corresponds to the same polymorph and its structure is almost identical to those at room temperature (Figure 3). In crystal of planar **5a** molecules are assembled by weak C-H...N contacts (H...N 2.4 Å) with nitrogen atoms of oxadiazole ring. These layers in turn are assembled in two 3-dimensional frameworks by the stacking interactions with C...C and C...N contacts equal to 3.52 and 3.42 Å.

According to XRD the rhenium atom in complex **9a** has been characterized by the expected octahedral environment with two CO groups and **5a** ligand in equatorial plane and CO and Br ones in apical positions (Figure 4). The comparison of bond lengths in this ligand and complexes has clearly showed that coordination led to some elongation of N-C bonds in phenantroline moiety. The analysis of crystal packing has revealed that in **9a** the presence of Re(CO)₃Br fragment has excluded the formation of staking interaction between ligands and various contacts of X... π types were realized. One can fetch out the Br... π , CO... π and finally O(1)... π ones (Figure 5). In the case of the latter O(1) atom has participated in the formation of rather rare symmetric η^6 -mode for O... π interaction with O...C distances varying in the range of 3.040-3.068(6)Å.

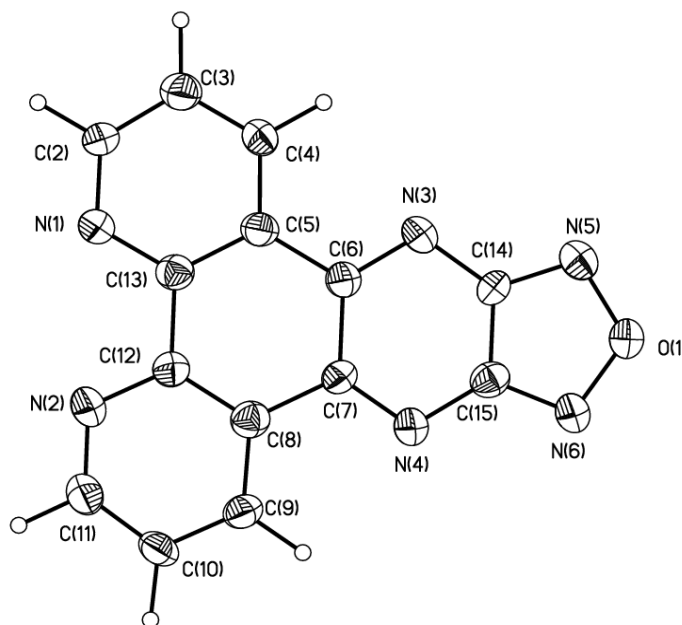


Figure 3. The general view of **5a** in crystal in representation of non-hydrogen by probability ellipsoids of atomic displacements ($p=50\%$). Selected bond lengths (Å): N(1)-C(2) 1.321(6), N(1)-C(13) 1.347(6), N(2)-C(11) 1.321(6), N(2)-C(12) 1.347(6), N(3)-C(6) 1.313(6), N(3)-C(14) 1.356(6), N(4)-C(7) 1.296(6), N(4)-C(15) 1.363(6), N(5)-C(14) 1.319(6), N(5)-O(1) 1.376(5), N(6)-C(15) 1.319(6), N(6)-O(1) 1.374(5).

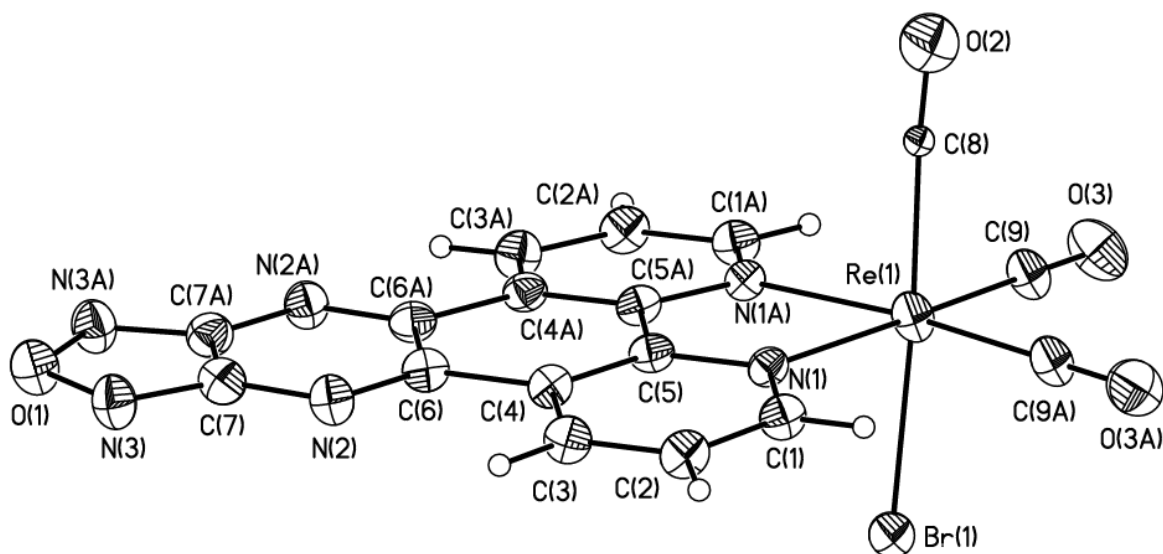


Figure 4. The general view of **9a** in crystal in representation of non-hydrogen by probability ellipsoids of atomic displacements ($p=50\%$). Molecule occupy the special position – mirror plane passing through Re(1), Br(1), C(8), O(2) and O(1) atoms. The disorder has caused by superposition of CO and bromide atoms in apical positions (see experimental part) was omitted for clarity. Selected bond lengths (\AA): Re(1)-C(8) 2.047(10), Re(1)-C(9) 1.929(7), Re(1)-N(1) 2.165(5), Re(1)-Br(1) 2.5408(16), O(1)-N(3) 1.383(7), N(1)-C(1) 1.347(8), N(1)-C(5) 1.356(8), N(2)-C(6) 1.308(8), N(2)-C(7) 1.352(9).

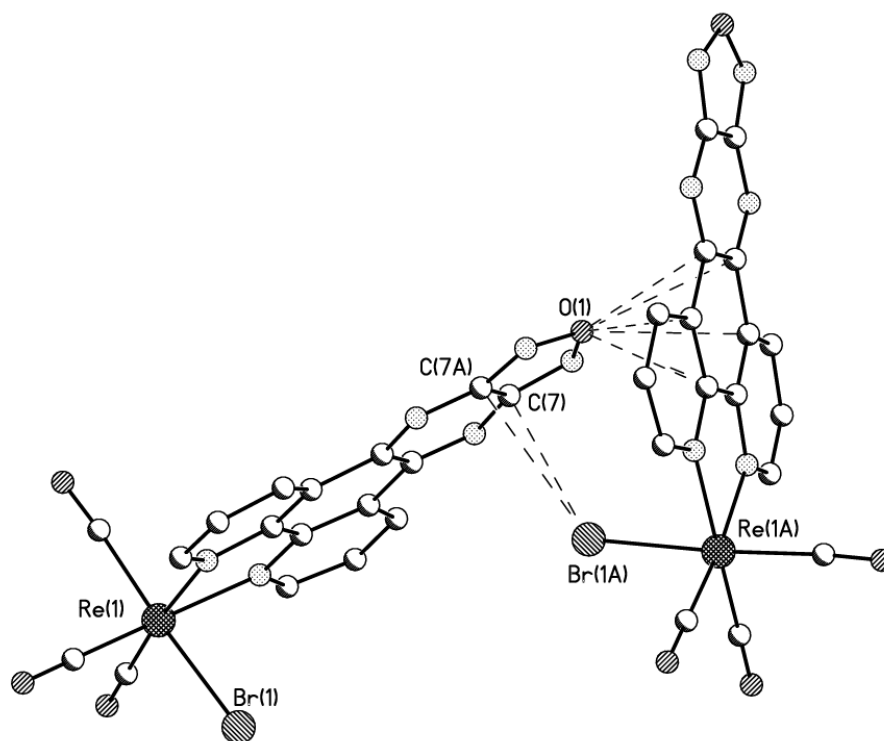


Figure 5. Molecular interactions of **9a** molecular in crystal in representation of non-hydrogen by probability ellipsoids of atomic displacements ($p=50\%$).

Photophysical properties. The absorption spectrum of **9a** in degassed DMSO solution is presented in Figure 6. The first maximum at 345 nm ($\epsilon = 1.18 \cdot 10^4 \text{ L mol}^{-1} \text{ cm}^{-1}$) can be assigned to spin-allowed $\pi \rightarrow \pi^*$ transitions in organic ligand, while strong band at 478 nm ($\epsilon = 1.07 \cdot 10^4 \text{ mol}^{-1} \text{ cm}^{-1}$) was tentatively ascribed to the triplet metal-to-ligand charge transfer ($^3\text{MLCT}$ state)¹⁵ The luminescence of **9a** in solid state at 300 K was negligible, while for degassed solutions in DMSO at the same temperature it can be seen by naked eye. The observed quenching of luminescence in the solid state can be the consequence of the above mentioned intermolecular contacts. The emission and excitation spectra for the $8 \cdot 10^{-4}$ M solution in DMSO are represented in Figure 7.

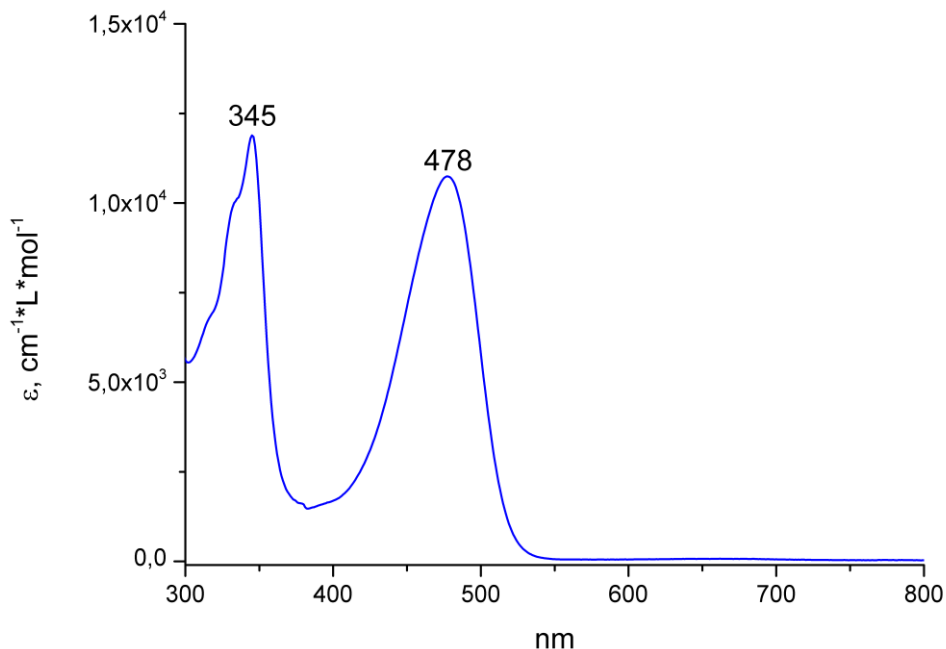


Figure 6. Absorption spectrum of $5 \cdot 10^{-5}$ M solution of **9a** in DMSO.

Upon short wavelength excitation (360 nm) a strong emission of ligand at 412 nm has been observed along with weak phosphorescence of $^3\text{MLCT}$ state at 640 nm. One can assume from the analysis of excitation spectrum, that effective pumping of $^3\text{MLCT}$ state was achieved by radiation with wavelength around 478 nm. This wavelength was matching maximum in absorption spectrum which was assigned to $\pi \rightarrow ^3\text{MLCT}$ transition. Indeed, if 485 nm excitation radiation has been used, the intensity of $^3\text{MLCT}$ luminescence increased dramatically. This observation has confirmed correctness of ascription of absorption band around 478 nm to $\pi \rightarrow ^3\text{MLCT}$ transition. Characteristic lifetime of the excited state in the solution at 300 K was 186 ns ($\pm 15\%$) and absolute quantum yield was 0.016 ± 0.003 . These data were in good agreement with values reported previously for other Re(I) diimine complexes with predomination of $^3\text{MLCT}$ phosphorescence.⁷

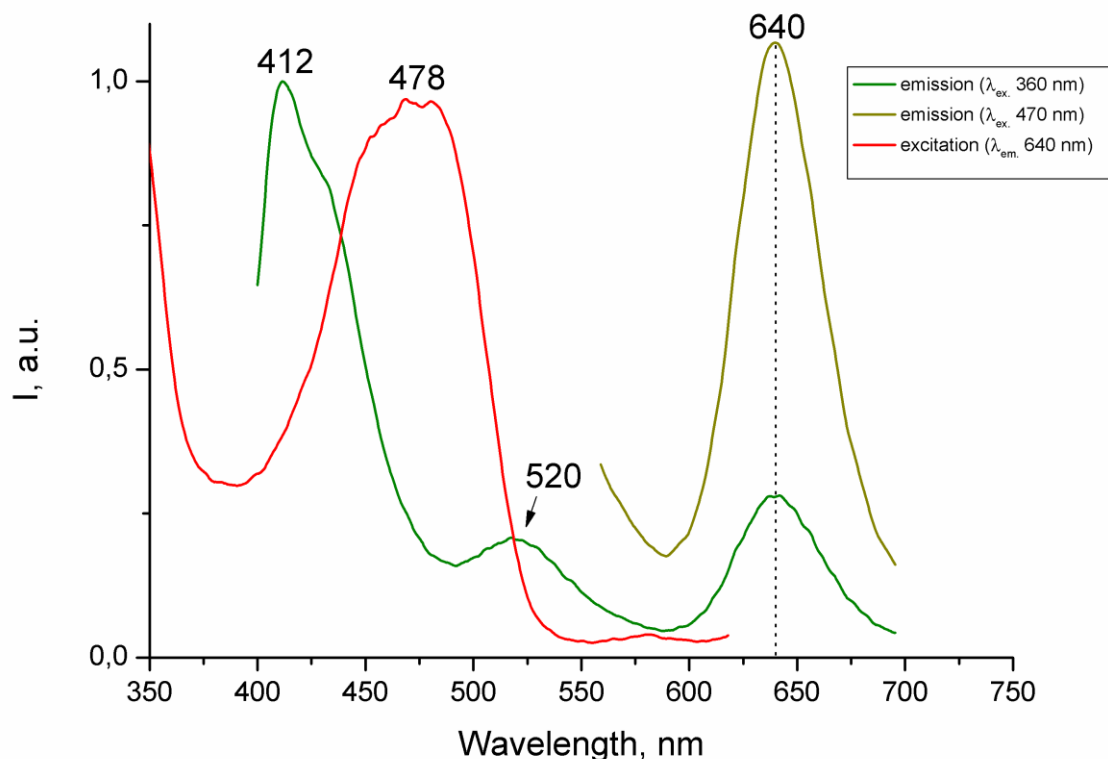


Figure 7. Excitation and emission spectra of $8 \cdot 10^{-4}$ M solution of **9a** in DMSO.

A very specific property of phosphors based on heavy *d*-elements, and among them for rhenium complexes, is their tendency to self-quenching or concentration quenching.¹ That means significant decreasing of quantum yields in pure film of complexes or in high concentration solutions. This problem is usually overcome by dissolution of emission material by so-called host material. Typical concentration of dopant in host material may vary from 1-2% up to 50% by weight.³ In this work TPD (*N,N'*-bis(3-methylphenyl)-*N,N'*-diphenylbenzidine) has been used as a host material. Optimal concentration of complex **9a** was found around 20%. It should be noted that OLED structures have been not fully optimized and this part of the work is still in progress. OLED structures have been prepared by coevaporation of components of pretreated glass-ITO (Indium-Tin Oxide)-PEDOT:PSS substrate. The architecture of OLED structures is presented in Figure 8.

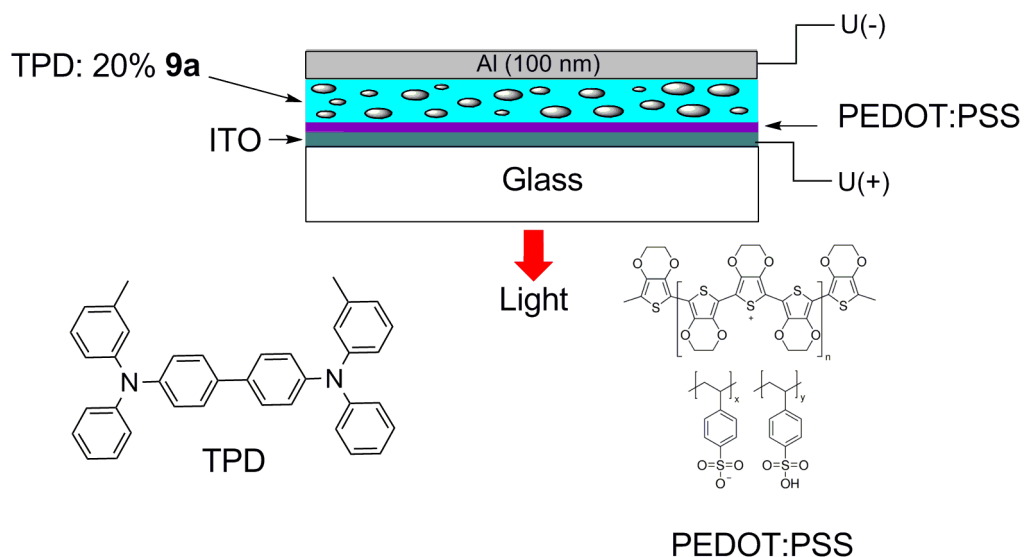


Figure 8. OLED structure and composition of intermediate layers.

OLED has been operated under relatively high voltage (turn-on voltage was 6 V) and has emitted red light as a broad band with maximum around 720 nm. The maximum brightness was 320 cd/m² at 13 V. Emission spectrum and current-voltage diagram were presented in the Figure 9 and Figure 10 respectively. The maximum in electroluminescent spectrum has been red-shifted related to maximum in photoluminescent spectrum due to Stark splitting in the electric field. The overall brightness was not high but it can be sufficiently increased by careful structure optimization.

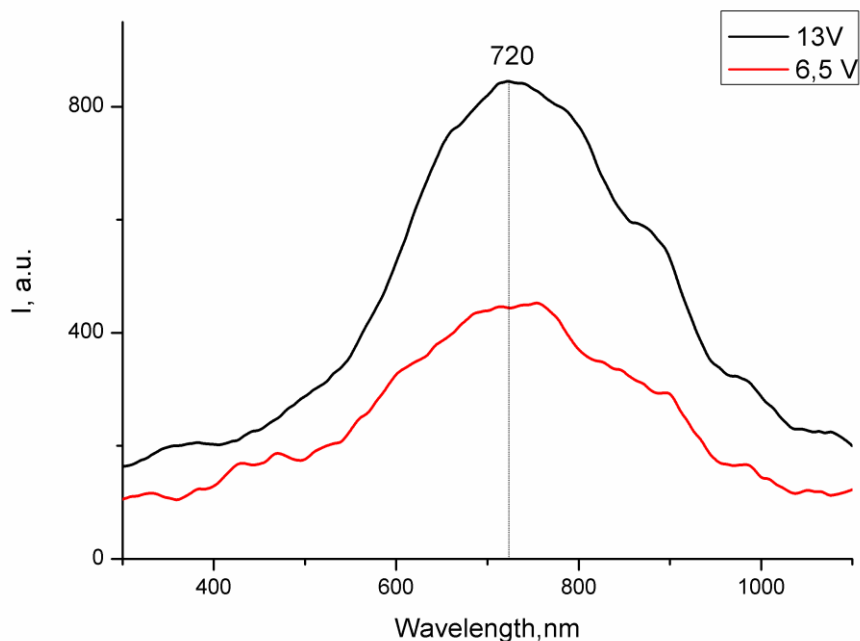


Figure 9. Electroluminescence spectra for OLED structure.

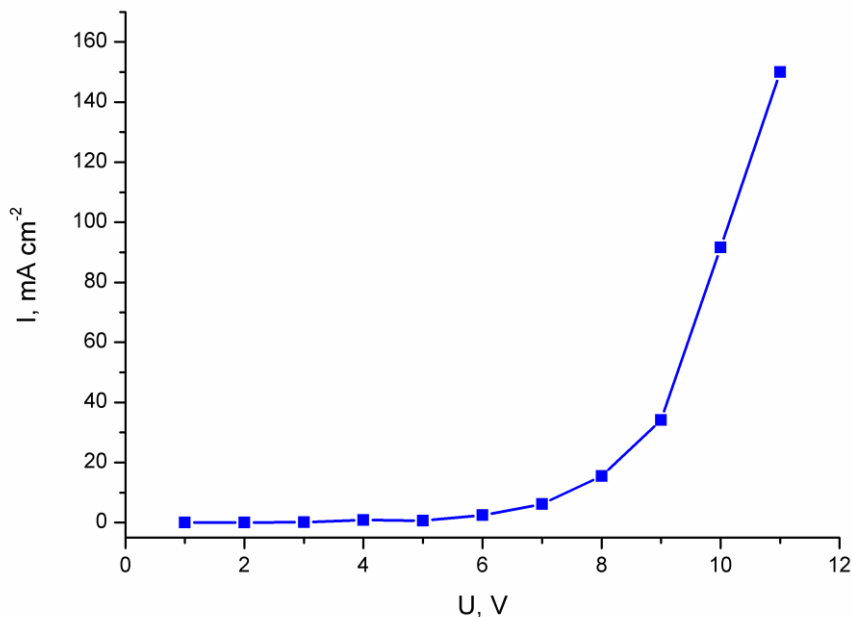


Figure 10. Current-voltage diagram for OLED structure.

Conclusions

An efficient synthetic protocol has been developed for the preparation of [1,2,5]chalcogenadiazolo[3',4':5,6]pyrazino[2,3-*f*][1,10]phenanthrolines by interaction of 1,2,5-chalcogenadiazole-3,4-diamine and 1,10-phenanthroline-5,6-dione in boiling AcOH. The first Re(I) bromotricarbonyl complex bearing [1,2,5]oxadiazolo[3',4':5,6]pyrazino[2,3-*f*][1,10]phenanthroline (**5a**) as a ligand was synthesized. Crystal structure, photo- and electroluminescent properties of *fac*-bromotricarbonyl([1,2,5]oxadiazolo[3',4':5,6]pyrazino[2,3-*f*][1,10]phenanthroline) rhenium (I) (**9a**) were investigated.

Experimental Section

General. The reagents were purchased from the commercial sources and used as received. Solvents were purified by distillation from the appropriate drying agents. 3,4-Diamino-1,2,5-thiadiazole¹⁶ was prepared by previously described method. Elemental analyses were performed on Perkin Elmer 2400 Elemental Analyser. Melting points were determined on a Kofler hot-stage apparatus and were uncorrected. ¹H NMR spectra were taken with a Bruker AM-300 spectrometer (at frequency of 300.1 MHz) in DMSO-*d*₆ solutions, with TMS as the standard. *J* values are given in Hz. MS spectra (EI, 70 eV) were obtained with a Finnigan MAT INCOS 50 instrument. High-resolution MS spectra were measured on a Bruker microTOF II instrument using electrospray ionization (ESI). IR spectra were measured with a Specord M-80 instrument in KBr pellets. Impurity concentrations were measured by a NexION 300D (Perkim Elmer) inductively coupled plasma mass-spectrometer. UV-VIS absorption spectra were recorded on a Varian Cary-100 Scan instrument. Luminescent

spectra were obtained on a Fluorolog FL3-22 (Horiba–Jobin–Yvon) spectrofluorimeter equipped by 450 W xenon lamp and standard Hamamatsu R-928 PMT. All spectra were corrected for instrumental responses. Quantum yields were measured by absolute method on the same set-up using integration sphere (Quata- ϕ) covered with Spectralone in 1 cm sealed quartz cuvettes for degassed solutions in DMSO.

General procedure for the synthesis of [1,2,5]chalcogenadiazolo[3',4':5,6]pyrazino[2,3-f][1,10]phenanthrolines (5). A mixture of 1,2,5-chalcogenadiazole-3,4-diamine (1.0 mmol) **2** and 1,10-phenanthroline-5,6-dione (230 mg, 1.1 mmol) **1** in AcOH (5.0 ml) was refluxed for 2 h and cooled. Precipitate was filtered, washed with Et₂O (3 x 5ml) and dried. The filtrate was evaporated, the residue was triturated with Et₂O (5ml), the additional precipitate was filtered and dried.

[1,2,5]Oxadiazolo[3',4':5,6]pyrazino[2,3-f][1,10]phenanthroline (5a). Yellow crystals, yield 92%, Mp > 250 °C (decomp.). ¹H NMR (DMSO-*d*₆): δ_{H} 7.80 (dd, 2H, Ar, J_1 8.2 Hz, J_2 4.5 Hz); 9.25 (m, 4H, Ar); 9.43 (dd, 2H, Ar, J_1 8.1 Hz, J_2 1.6 Hz). IR (KBr, cm⁻¹): 3071 (C-H), 1579, 1561, 1508, 1465, 1442, 1417, 1341, 1315, 1129, 1079, 1036, 1019, 872, 850, 825, 742. MS (EI, 70 eV) *m/z* (%): 274 (M⁺, 100), 244 (67), 192 (88), 165 (33). Anal. Calcd. for C₁₄H₆N₆O: C 61.32; H 2.21; N 30.65; found : C, 61.15; H, 2.10; N, 30.38%. HRMS (ESI), *m/z*: 297.0496 [M+Na]⁺ (calc. for C₁₄H₆N₆O, *m/z*: 297.0495).

[1,2,5]Thiadiazolo[3',4':5,6]pyrazino[2,3-f][1,10]phenanthroline (5b). Yellow crystals, yield 82%, Mp > 250 °C(decomp.). IR (KBr, cm⁻¹): 3081 (C-H), 1576, 1535, 1493, 1404, 1326, 1130, 1080, 1037, 897, 813, 738. MS (EI, 70 eV) *m/z* (%): 290 (M⁺, 100), 263 (16), 244 (8), 232 (8), 205 (14), 192 (10). Found (%): C, 57.75; H, 2.01; N, 28.64. Anal. Calcd. for C₁₄H₆N₆O: C₁₄H₆N₆S (%): C 57.92; H 2.08; N 28.95; found: C, 57.75; H, 2.01; N, 28.64 %. HRMS (ESI), *m/z*: 313.0247 [M+Na]⁺ (calc. for C₁₄H₆N₆S, *m/z*: 313.0267).

Fac-Bromotricarbonyl([1,2,5]oxadiazolo[3',4':5,6]pyrazino[2,3-f][1,10]phenanthroline) rhenium (I) (9a). Heavy wall Pyrex tube (overall volume 20 mL), equipped with Teflon coated stirring bar, was charged with 44.7 mg (0.11 mmol) Re(CO)₅Br, 10 mL of dry toluene and 28 mg (0.1 mmol) of **5a**. The resulted suspension was purged by steam of Ar for 10 min, sealed, wrapped with aluminum foil to protect from light and heated with stirring in oil bath at 120 °C (bath temperature) for 5h. Then reaction tube was slowly cooled to RT (with bath), dark red crystals were collected, filtered, washed with toluene (5 mL), hot EtOH (5mL) and hexane (5mL) and dried *in vacuo* (0.1 Torr, 40 °C) to a constant weight. Yield – 54.7 mg (87%). Mp > 300 °C(decomp.). Anal. Calcd. for C₁₇H₆BrN₆O₄Re (%): C 32.70; H 0.97; N 13.46; Found:C 32.76; H 1.06; N 13.39%. HRMS (ESI), *m/z*: 624.3771 [M]⁺ (calc. for C₁₇H₆BrN₆O₄Re *m/z*: 624.3786). Inorganic purity - 99.97% (ICP-MS).

X-ray crystallography. X-ray diffraction data were collected on a APEX II DUO CCD diffractometer using molybdenum radiation [λ (MoK α) = 0.71072 Å, ω -scans] for **5a** and **9a** at 110 K. The substantial redundancy in data allowed empirical absorption correction to be applied with SADABS by multiple measurements of equivalent reflections. The structures were solved by direct methods and refined by the full-matrix least-squares technique against F^2 in the anisotropic-isotropic approximation. In **9a** the analysis of the Fourier maps has revealed a disorder that is a superposition of bromine atom and C=O group in both apical positions of the rhenium polyhedron. The occupancies of two bromine atoms Br(1) and Br(1') were equal to 0.646(2) and 0.354(2) and corresponding values for C(8)O(2) and C(8')O(2') were 0.354(2) and 0.646(2). The positional and atomic displacement parameters of these two components were refined with the constraints on the Re-Br, Re-C and C-O bond length (DFIX) and atomic anisotropic displacement parameters (EADP). Hydrogen atoms in all structures were placed in calculated positions and refined within the riding model. All calculations were performed with the SHELXTL software package.¹⁷ Crystal data and structure refinement parameters are listed in Table 1 (Supporting Information). Crystallographic data for the structures reported in this paper have been deposited to the Cambridge Crystallographic Data Centre as supplementary no.: CCDC- 1537819 (for **5a**) and

CCDC- 1537820 (for **9a**). These data can be obtained free of charge from The Cambridge Crystallographic Data via www.ccdc.cam.ac.uk/data_request/cif.

OLED fabrication and characterization. Multilayer OLED devices were fabricated by layer-by-layer vacuum thermal deposition ($<10^{-5}$ Pa) on a glass substrate (20x30x3 mm,) covered by ITO/ PEDOT:PSS conducting layer. PEDOT:PSS (hole injection material) solution (high conductivity), electronic grade, was purchased from Aldrich. It was spin-coated on the clean ITO surface (substrate initial resistance was 20 Ω /sq) and annealed at 100 °C at Ar atmosphere for 30 min. Then substrate was transferred to vacuum evaporation chamber. TPD was used as hole hole transport layer and a host material. Layer materials were coevaporated from individual resistance heated boats. Deposition rates and thicknesses of layers were monitored by an oscillating quartz monitor. The deposition rates of each layer were no more than 0.03 nm \times s $^{-1}$. The OLED structure was ITO-PEDOT:PSS/ TPD:**9a** (20%)(20 nm) /Al (100 nm). EL spectra of the devices were measured by a MayaPro 100 spectrometer (Ocean Optics, Inc.).

Acknowledgements

This work was financially supported by the Russian Science Foundation (grant no. 15-13-10022), RFFI 16-03-00832 A (KAL and IVT) and by the Ministry of Education and Science of the Russian Federation (South Ural State University, grant no. 4.9651.2017-2017115-Г3). Technological part of this work (OLED fabrication) was partially supported by the Russian Science Foundation, grant no. 14-13-01074 . We are grateful to Prof. I. Ch. Avetissov and Dr. A. Mozhevitina (D. Mendeleev University of Chemical Technology of Russia) for the performing of ICP-MS experiments.

Supplementary Material

Table of crystal data and structure refinement parameters for the compounds **5a** and **9a** and corresponding crystallographic data files (cif) can be found in the Supplementary Material.

References

1. Buckley, A. Organic Light-Emitting Diodes (OLEDs). Woodhead Publishing, Cambridge, **2013**, pp. 3-169. <http://dx.doi.org/10.1533/9780857098948.frontmatter>
2. Mohd-Nasir, S. N. F.; Sulaiman, M. Y.; Ahmad-Ludin, N.; Ibrahim, M. A.; Sopian, K.; Mat-Teridi, M. A. *Int. J. Photoenergy* **2014**, 2014, 1-12. <http://dx.doi.org/10.1155/2014/370160>
3. Yersin, H. Highly Efficient OLEDs with Phosphorescent Materials. Wiley-VCH Verlag, Weinheim, **2008**, 131-216. <http://dx.doi.org/10.1002/9783527621309.fmatter>
4. Goncalves, M. R.; Frin K.P.M. *Polyhedron* **2015**, 97, 112-117. <http://dx.doi.org/10.1016/j.poly.2015.05.007>
5. Chi, Y.; Tong, B.; Chou, P.-T. *Coord. Chem. Rev.*, **2014**, 281, 1-25. <http://dx.doi.org/doi:10.1016/j.ccr.2014.08.012>

6. Velmurugan, G.; Ramamoorthi, B. K.; Venuvanalingam, P. *Phys.Chem.Chem.Phys.* **2014**, *16*, 21157-21171.
<http://dx.doi.org/10.1039/C4CP01135J>
7. Wrighton, M; Morse, D. L. J. *Am. Chem. Soc.* **1974**, *96*, 998–1003.
<http://dx.doi.org/10.1021/ja00811a008>
8. Chan, W. K.; Ng P. K.; Gong, X.; Hou, S. *Appl. Phys. Lett.* **1999**, *75*, 3920-3922.
<http://dx.doi.org/10.1063/1.125494>
9. Li, X.; Zhang, D.; Li, W.; Chu, B.; Han, L.; Zhu, J.; Su, Z.; Bi D.; Wang, D., Yang, D.; Chen, Y. *Appl. Phys. Lett.* **2008**, *92*, 083302.
<http://dx.doi.org/10.1063/1.2888767>
10. Si, Z.; Li, J.; Li, B.; Zhao, F.; Liu, S.; Li, W. *Inorg. Chem.* **2007**, *46*, 6155-6163.
<http://dx.doi.org/10.1021/ic061645o>
11. Si, Z.; Li, J.; Li, B.; Hong, Z.; Lu, S.; Liu, S.; Li, W. *Appl. Phys. A* **2007**, *88*, 643–646.
<http://dx.doi.org/10.1007/s00339-007-4003-z>
12. Peng, B.; Chena, X.; Dua, K.-J.; Yua, B.-L.; Chaoa, H.; Ji, L.-N. *Spectrochim. Acta A* **2009**, *74*, 896–901.
<http://dx.doi.org/10.1016/j.saa.2009.08.031>
13. Yu, H.; Huang, S.; Chao, H.; Ji, L. *J. Inorg. Biochem.* **2015**, *149*, 80–87.
<http://dx.doi.org/10.1016/j.jinorgbio.2015.02.020>
14. MacQueen, D. B.; Schanze K. S. *J. Am. Chem. Soc.* **1991**, *113*, 7470–7479
<http://dx.doi.org/10.1021/ja00020a003>
15. Wang, C.; Lystrom, L.; Yin, H.; Hetu, M.; Kilina, S.; McFarland, S. A.; Sun, W. *Dalton Trans.* **2016**, *45*, 16366-16378.
<http://dx.doi.org/10.1039/C6DT02416E>
16. Konstantinova L. S.; Bobkova, I.E.; Nelyubina, Y. V.; Chulanova, E. A.; Irtegova, I. G.; Vasilieva, N. V.; Camacho, P. S.; Ashbrook, S. E.; Hua, G.; Slawin, A. M. Z.; Woollins, J. D.; Zibarev, A. V.; Rakitin, O. A. *Eur. J. Org. Chem.* **2015**, 5585–5593.
<http://dx.doi.org/10.1002/ejoc.201500742>
17. Sheldrick. G. M. *Acta. Cryst.* **2008**, *A64*, 112-122
<http://dx.doi.org/10.1107/S0108767307043930>